

Enantiopure Double *ortho*-Oligophenylethynylene-Based Helical Structures with Circularly Polarized Luminescence Activity

Pablo Reiné⁺,^[a] Ana M. Ortuño⁺,^[a] Sandra Resa,^[a] Luis Álvarez de Cienfuegos,^[a] María Ribagorda,^[b] Antonio J. Mota,^[c] Sergio Abbate,^[d] Giovanna Longhi,^{*,[d]} Delia Miguel,^{*,[e]} and Juan M. Cuerva^{*,[a]}

In this paper, we describe the optical and chiroptical properties of an enantiopure multipodal *ortho*-oligophenylethynylene (*S,S,S,S*)-1 presenting four chiral sulfoxide groups at the extremes. The presence of these groups together with alkynes allows the coordination with carbophilic Ag(I), and/or oxophilic Zn(II) cations, yielding double helical structures in an enantiopure way. In this sense, different behaviors in absorption, fluorescence, ECD and CPL spectra have been found depending on the stoichiometry and nature of the metal. We have observed that Zn(II) coordination favors an intensity increase of

the electronic circular dichroism (ECD) spectra of compound (*S,S,S,S*)-1 yielding an *M*-helicity in the *ortho*-oligophenylene ethynylene (*o*-OPE) backbone. On the other hand, ECD spectra of final Ag(I) complex shows two different bands with an opposite sign to the free ligand, thus giving the *P*-helical isomer. In addition, circularly polarized luminescence (CPL) exhibit an enhanced intensity and negative sign in both complexes. Computational studies were also carried out, supporting the experimental results.

1. Introduction

Mimicry of biotic enantiopure helical nanostructures has been used as a model to understand their function in nature.^[1,2] Among all the variety of chemical structures synthesized, helicenes have attracted the attention of many groups as they combine helical geometry and π -conjugation. This combination result in remarkable chiroptical properties, as electronic circular dichroism (ECD) and circularly polarized luminescence (CPL).^[3,4] This last property of emissive chiral species is based on the biased emission of left or right-handed circularly polarized light.

CPL is usually characterized by the dimensionless parameter g_{lum} , defined as $g_{lum} = 2(I_L - I_R)/(I_L + I_R)$, called luminescence dissymmetry ratio. It provides a quantitative estimation of circularly polarized emitted radiation over total emitted radiation. As in the case of ECD, the property relies on the existence of a helical movement of electrons during the corresponding transition owing to the existence of a non-null electronic (μ) and magnetic (m) dipole transition vectors. Consequently, enantiopure helical structures usually result in intense CPL emissions.

[a] Dr. P. Reiné,⁺ A. M. Ortuño,⁺ Dr. S. Resa, Dr. L. Álvarez de Cienfuegos, Prof. J. M. Cuerva
Department of Organic Chemistry
Unidad de Excelencia de Química
University of Granada
Faculty of Science, C. U. Fuentenueva
18071 Granada (Spain)
E-mail: jmcuerva@ugr.es

[b] Dr. M. Ribagorda
Organic Chemistry Department
Department of Organic Chemistry
Universidad Autónoma de Madrid
C/Francisco Tomás y Valiente n° 7
Cantoblanco, 28049 Madrid (Spain)

[c] Dr. A. J. Mota
Department of Inorganic Chemistry
Unidad de Excelencia de Química
University of Granada
Faculty of Science, C. U. Fuentenueva
18071 Granada (Spain)

[d] Prof. S. Abbate, Prof. G. Longhi
Department of Molecular and Translational Medicine
Istituto Nazionale di Ottica – CNR, Brescia Research Unit
Università di Brescia
Via Branze 45, 25123 Brescia (Italy)
E-mail: giovanna.longhi@unibs.it

[e] Dr. D. Miguel
Physical Chemistry Department
Unidad de Excelencia de Química
University of Granada
Faculty of Pharmacy, C. U. Cartuja
18071 Granada (Spain)
E-mail: dmalvarez@ugr.es

[⁺] These authors contributed equally to this work.



Supporting information for this article is available on the WWW under <https://doi.org/10.1002/cptc.202100160>



An invited contribution to a Special Collection on Circularly Polarized Luminescence.



© 2021 The Authors. ChemPhotoChem published by Wiley-VCH GmbH. This is an open access article under the terms of the Creative Commons Attribution Non-Commercial License, which permits use, distribution and reproduction in any medium, provided the original work is properly cited and is not used for commercial purposes.

Recently, there has been a growing interest in fusing multiple helices in special arrangements^[5,6] and also in analyzing the consequences in the values of the chiroptical properties.^[7–9] Among all the variety of multiple helicenes prepared, double helicenes are the simplest and most studied ones, including carbo[5]- to [8]helicenes and hetero[4]- to [7] helicenes and also metallo-multihelicenes.^[10] Although in many cases g_{lum} factors are not reported, the highest values obtained to date correspond to double hetero[6]helicenes described by Tanaka,^[11] with $g_{lum} = 1.1 \times 10^{-2}$ and 2.8×10^{-2} , and a Zn(II) metallohelicene^[12] ($g_{lum} = 2.2 \times 10^{-2}$). Despite the undeniable interest of these derivatives, the number and structural variability of multiple helicenes reported to date is still limited.

Apart from helicenes, which are conformationally blocked, the huge chemical space beyond natural building blocks has also allowed the flourishing of a plethora of abiotic (usually aromatic) helical structures based on dynamic folding processes (foldamers).^[13,14] The control of the folding process is therefore a key point which determines their properties. In this sense, many strategies have been developed for such control, including the interaction with metals.^[15] In the last years, our group has been interested in *o*-OPEs as versatile scaffolds to develop architectures with remarkable (chir)-optical responses, in particular, as CPL emitters.^[16,17] These structures present some advantages over parent helicenes. Thus for example, synthetic routes allow the preparation of enantiopure derivatives with up to four complete helical loops and high g_{abs} and g_{lum} values in ECD and CPL spectra in the range of $1\text{--}2.5 \times 10^{-2}$.^[18]

A characteristic feature of *o*-OPEs compared to other foldamers is the appetite of such alkyne arrangement for carbophilic cations, as Ag(I). Based on that, we have described helical structures due to the selective Ag(I)-alkyne interactions in *o*-OPEs, thus providing hybrid organic-inorganic structures mimicking a coaxial wire structure.^[16,19] Moreover, a switchable system^[20] can be achieved by controlling the bias of the *P/M* conformational equilibrium in solution. Within this context, one of the most appealing approaches is based on the incorporation of an enantiopure sulfoxide as chiral inductor in the structure.^[21,22] Such functionality plays a dual role: i) inducing a preorganization of the helical conformation via a rupture of the energetically degenerated *P/M* conformations, and ii) controlling the *o*-OPE-cation binding interaction. Thus, for example, CPL active systems exhibiting both roles have been described with a complementary OFF/ON switching event produced in the presence of oxophilic metals, resulting in highly emissive complexes with quantum yields from 38 to 84% and g_{lum} values up to 0.7×10^{-2} .^[23]

Considering our previous experience and the growing interest in multiple helicene systems, in the present work we explore more complex architectures based on OPEs, including different binding possibilities for oxophilic and carbophilic metals, in order to obtain different CPL profiles. To this end, a multipodal ligand (*S,S,S,S*)-1 containing four enantiopure (*S*)-sulfinyl groups has been synthesized and tested (Figure 1). It presents different binding sites (six alkynes and four sulfoxides) thus allowing different potential geometries and chiroptical responses. Compound (*S,S*)-2 containing only two (*S*)-sulfinyl

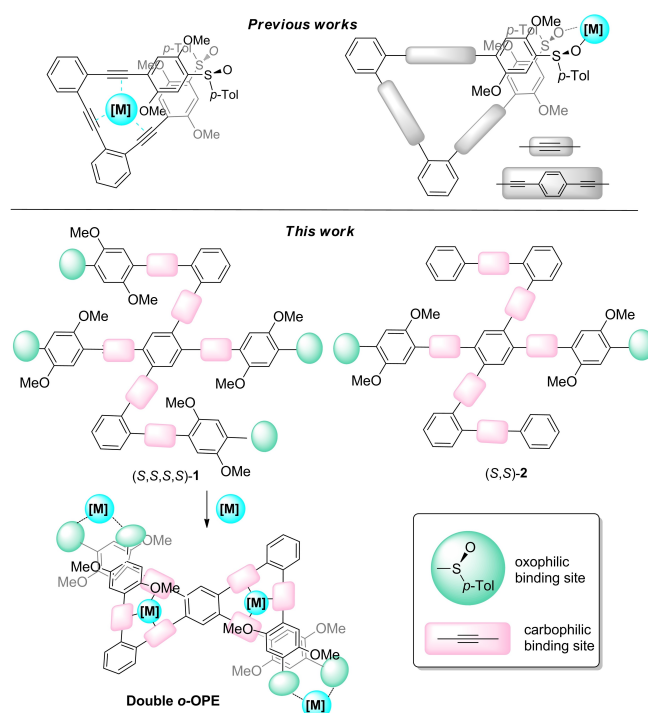


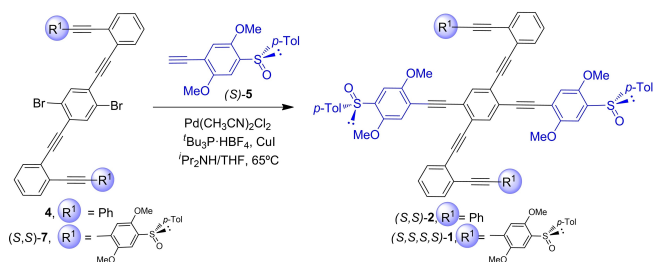
Figure 1. Previously developed *o*-OPEs (top) and multipodal structures with carbophilic and oxophilic binding sites described in this work (bottom).

groups is used as a model compound. As expected, the presence of the enantiopure sulfoxide groups imposes helical chirality to the whole structure with a prevalent handedness. Nevertheless, their behavior towards carbophilic (Ag(I)) and prototypical oxophilic metal (Zn(II)) is not identical. The corresponding complexes have been fully characterized, showing that handedness depends on the metal. Different CPL behaviors are observed owing to the rich binding possibilities of these systems.

2. Results and Discussion

Compounds (*S,S,S,S*)-1 and (*S,S*)-2 were prepared using successive Sonogashira and alkynyl deprotection reactions as the key steps (Scheme 1). Enantiopure 1,4-dimethoxy aryl substituted bisaromatic sulfoxide (*S*)-5 was chosen as homochiral sulfinyl group due to its well established ability to adopt a rigid *S-cis* conformation which could be able to induce a defined orientation of the overall system.^[24] Thus, we prepared precursors 4 and (*S,S*)-7 from simple and commercially available dihaloaryl derivatives with trimethylsilyl acetylene or phenyl-acetylene followed by removal of the protecting silyl group. Then, both intermediates were coupled with (*S*)-5, affording model compound (*S,S*)-2 and multipodal structure (*S,S,S,S*)-1 in 63% and 40% yield respectively (see SI for details).

With both compounds on hands we analyzed their photo-physical properties, in terms of absorbance, fluorescence, quantum yields and fluorescence lifetimes. To be compatible with the analysis of the complexes in terms of solubility the



Scheme 1. Synthetic route for the preparation of compounds (S,S,S,S)-1 and (S,S)-2.

studies were carried out in 95:5 mixture of CH₂Cl₂:acetone solutions at $\approx 25 \mu\text{M}$ concentrations. Absorbance spectra profiles of both derivatives are similar, presenting two main bands at 320 nm and 350 nm, with a shoulder around 390 nm, more pronounced in the case of (S,S,S,S)-1. Regarding emission properties, (S,S)-2 presents a maximum, slightly redshifted in comparison with (S,S,S,S)-1, and a noticeable shoulder at 535 nm (Figure 2a).

These photophysical techniques were also used to evaluate the coordination capabilities of these compounds in the presence of AgBF₄ and Zn(OTf)₂ as Ag(I) and Zn(II) sources respectively, both salts having non-coordinating counteranions. While no changes were observed after titrations with either Ag(I) or Zn(II) salts in model compound (S,S)-2, absorption and fluorescence spectra of derivative (S,S,S,S)-1 showed changes in the shape and intensity of the bands when increasing the concentrations of both metals. As it can be seen in Figure 2b, the addition of 10 equivalents of AgBF₄ promotes a decrease in the intensity of both absorption and emission spectra, causing in addition a broadening of the bands (purple lines). In an opposite way, the coordination with Zn(II) favors the definition of the peaks and the increase of the intensity of the bands (green lines). Moreover, titration experiments showed different behavior between these metals at 3 μM concentration. In this sense, absorption spectra slightly change from one to 10 equiv-

alents of Ag(I) salt, whereas more drastic changes were observed after Zn(II) addition up to 2 equivalents and then remain almost identical. These differences are more remarkable in the emissive properties, where the ratio between the intensity of the two maxima evolves in opposite ways. In this sense, Ag(I) diminishes intensity at maximum absorption (450 nm) in favor of the shoulder at 530 nm, while the coordination with Zn(II) increases the intensity of the main peak by reducing the one corresponding to the broader band at 530 nm (see Figures S22 and S23 for titrations).

We also measured the quantum yields (QYs) of (S,S,S,S)-1 and (S,S)-2 in CH₂Cl₂ solutions using quinine sulfate as reference, resulting in high values of 65.2% and 49.5% respectively. As suggested in previous titration experiments, the QY of (S,S,S,S)-1 in the presence of Ag(I) diminishes to 20.4% but remains high for Zn(II) complex (48.5%). In addition, coordination process of both derivatives was also confirmed by NMR titrations, where spectra changed upon coordination with the salts. For model compound (S,S)-2 protons corresponding to methoxy groups of the sulfoxide moiety shifted to upfield when Zn(II) was added (Figure 3), whereas almost no changes were observed after Ag(I) addition. Moreover, aromatic protons move to lower chemical shifts in the presence of Zn(II) whereas shifted downfield when Ag(I) was used. Similar results were observed after Zn(II) complexation of compound (S,S,S,S)-1. On the other hand, good spectra could not be obtained for the corresponding Ag(I) titration owing to the formation of a precipitate after addition of the first equivalent. (see Figure S13). It is worth noting that the concentrations in NMR and photophysical measurements differ by orders of magnitude.

To obtain more information about the observed changes in fluorescence, especially the variable contribution of the shoulder present around 530 nm depending on the added metal, we decided to perform a deconvolution of the fluorescence spectra. To do this we carried out the Time Resolved Emission Spectra (TRES), using a 375 nm laser as excitation source. Figure 4 shows the spectra associated to the emissive species (SAEMS) present in the excited state for both compounds and the corresponding metal complexes. Model compound (S,S)-2 exhibits three different species with lifetimes of 4.3, 2.2 and 0.8 ns, although the one with the largest value is the main responsible of the shape and intensity of the emission spectra (Figure 4b). The existence of such lifetimes correlates with the presence in solution of different conformations unable to interconvert in the range of nanoseconds. On the other hand, TRES spectra of compound (S,S,S,S)-1 fitted to a bi-exponential function (Figure 4a), in which lifetime of around 4 ns exhibits in all cases the shoulder at 540 nm. Similar results were obtained for (S,S,S,S)-1 complexes (Figure 4c,d) although with a minor contribution of the species with a lifetime of 4 ns to the total emission spectra. The shoulder at 540 nm is present in the species with the shortest lifetime only when Ag(I) complex is formed. Although a clear interpretation of SAEMS is difficult, these results suggest the existence of different species in the excited state accordingly with the multipodal character of the ligand.

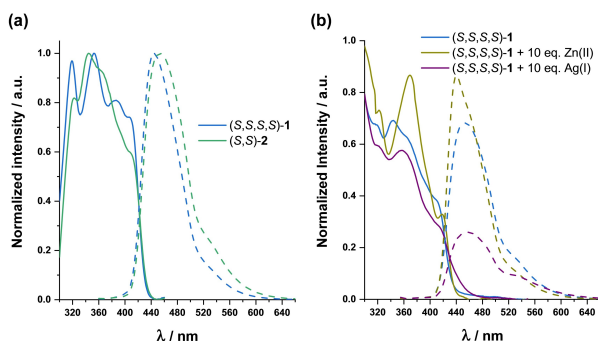
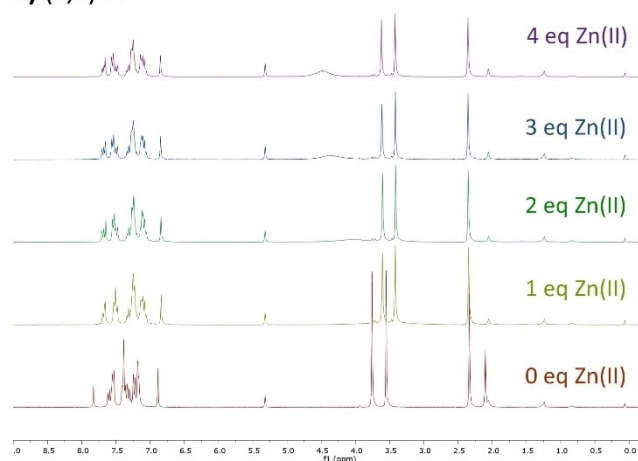


Figure 2. Normalized absorbance (solid) and fluorescence ($\lambda_{\text{exc}} = 345 \text{ nm}$, dotted line) spectra of a) compounds (S,S,S,S)-1 and (S,S)-2 in CH₂Cl₂ solutions and b) compound (S,S,S,S)-1 in the presence of an excess of Ag(I) and Zn(II) in 95:5 mixtures of CH₂Cl₂:acetone.

a) (S,S)-2



b) (S,S,S,S)-1

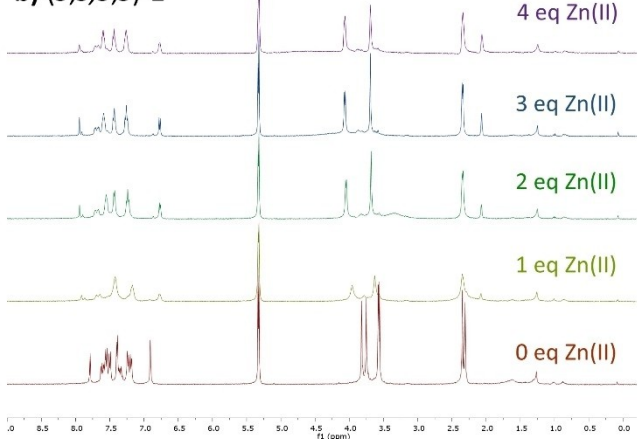


Figure 3. ^1H NMR spectroscopic titrations at room temperature of a) (S,S)-2 in CD_2Cl_2 and b) (S,S,S,S)-1 with $\text{Zn}(\text{OTf})_2$ in a 9:1 mixture of CD_2Cl_2 :acetone d_6 .

Next, we investigated the chiroptical properties of both compounds in absence and presence of metal salts in the ground and excited states. Compound (S,S,S,S)-1 ECD spectra presents one main negative band centered at around 420 nm ($\Delta\epsilon = -8 \text{ M}^{-1}\text{cm}^{-1}$), suggesting a prevalent *M* configuration of the helix. Nevertheless, the low ECD intensity calls also for a somehow disordered conformational landscape in which also non helicoidal geometries could contribute. This is in agreement with previous results of related systems. Compound (S,S)-2 shows a similar profile, with a slightly more intense ($\Delta\epsilon = -14 \text{ M}^{-1}\text{cm}^{-1}$) negative band at 410 nm. Unfortunately, the complex conformational space of these systems precludes a rigorous theoretical simulation of observed ECD. Coordination process was followed by means of chiroptical techniques owing to compound (S,S,S,S)-1 could be able to adopt a biased double helical structure strengthened by carbophilic interactions with alkynes, oxophilic functionalities of the sulfinyl groups or a combination of both kinds of interaction. Coordination with AgBF_4 and $\text{Zn}(\text{OTf})_2$ was then studied by ECD titrations of

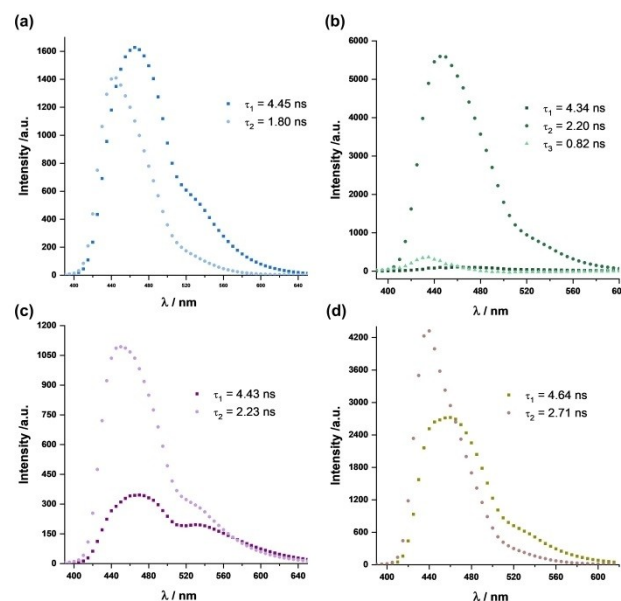


Figure 4. SAEMS spectra in CH_2Cl_2 solutions of compounds a) (S,S,S,S)-1, b) (S,S,S,S)-2; c) (S,S,S,S)-1 + 10 eq. $\text{Ag}(\text{I})$; d) (S,S,S,S)-1 + 10 eq. $\text{Zn}(\text{II})$.

25 μM solutions of (S,S,S,S)-1 in 95:5 CH_2Cl_2 :acetone mixtures. ECD spectra obtained after addition of one equivalent of both $\text{Ag}(\text{I})$ and $\text{Zn}(\text{II})$ salts (Figure 5) almost maintained unchanged the shape of the bands promoting mild intensification of the signal ($\Delta\epsilon \approx -12 \text{ M}^{-1}\text{cm}^{-1}$ for both complexes) with the maximum slightly red-shifted for the silver complex. This fact suggests that the average helicity of uncomplexed (S,S,S,S)-1 is retained in the complex with low $\text{Ag}(\text{I})$ and $\text{Zn}(\text{II})$ loadings, which is in accordance with the known fact that $\text{Ag}(\text{I})$ cations force the structure to planar after coordination with three alkynes. Only one equivalent is unable to satisfy availability for all the coordination sites of (S,S,S,S)-1 resulting in an almost disordered structure in which the original *M* helicity is retained. These results are clearly different from those observed with

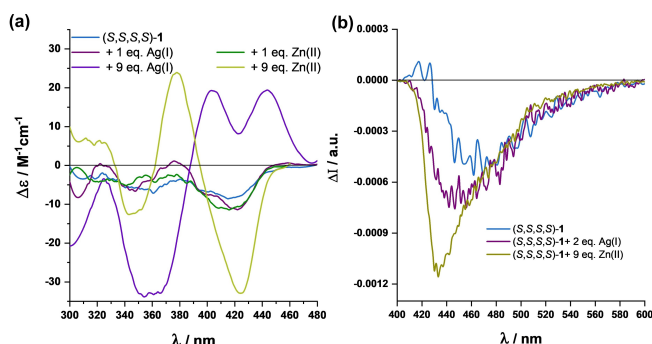


Figure 5. a) ECD and b) CPL spectra of compound (S,S,S,S)-1 in the absence (blue) and the presence of different amounts of $\text{Ag}(\text{I})$ (purple) and $\text{Zn}(\text{II})$ (green lines).

previously prepared simpler ligands.^[21,22] Beyond the first equivalent, a different behavior is observed in the titration. Increasing quantities of Ag(I) resulted in a continuous change from clearly negative bands (up to 2 equiv.) to a new spectrum with two positive maxima at 400 and 445 nm with similar intensities ($\Delta\epsilon = +20 \text{ M}^{-1} \text{ cm}^{-1}$) associated with an inversion of the helix with an excess of Ag(I) cation (Figure 5a).^[21] On the other hand, the use of up to 9 equivalents of $\text{Zn}(\text{OTf})_2$ promoted an outstanding increase of the ECD signal retaining both the sign and the shape, with a maximum at 425 nm ($\Delta\epsilon = -33 \text{ M}^{-1} \text{ cm}^{-1}$). The dissymmetry factor g_{abs} was also calculated for the lowest energetic band, being -8×10^{-4} for the ligand (S,S,S,S)-1 and -1.2×10^{-3} and $+2 \times 10^{-3}$ for Zn(II) and Ag(I) complexes respectively.

These experiments also allowed us to estimate the corresponding binding constants and the stoichiometry of both complexes (see Figures S24 and S25). Statistical fitting of Zn(II) coordination process shows a $\text{Zn}_2:(\text{S,S,S,S})\text{-1}$ stoichiometry and the corresponding global binding constant of $3.1 \times 10^8 \text{ M}^{-2} \pm 7.2\%$, in which the individual binding processes cannot be distinguished. Apparently, the coordination to the oxophilic sulfoxide groups in half of the symmetric molecule does not hamper the coordination in the other symmetric binding site. On the other hand, Ag(I) coordination phenomenon is much more complex due to up to six silver cations can be incorporated in the structure, considering the binding to the alkynes and sulfoxide groups. In this sense, the results were difficult to analyze and we got considerable errors in the fitting but still, and as we expected from previous results,^[22] we were able to distinguish two main different binding events. The first one is attributed to the incorporation of two Ag(I) atoms in the inner cavity defined by the alkynes and the second one, with a much lower binding constant, related with the coordination of additional Ag(I) cations to the sulfinyl functionalities (see SI for details). In addition, competitive experiments showed that Zn(II) complexes are more stable than Ag(I) ones, being Zn(II) cation able to displace the previously formed Ag(I)-complex.

We then analyzed the evolution of ECD spectra of compound (S,S)-2 in the presence of both Ag(I) and Zn(II), whose coordination has been previously demonstrated by NMR titrations. However, after treatment with 10 equivalents of each metal salt no significant changes were observed in the shape or the intensity of the signal, maintaining in both cases the negative sign of the main band (see Figure S26). This result suggests that the geometry of these complexes is similar to the free (S,S)-2.

We then measured the circularly polarized luminescence (CPL) spectra of derivative (S,S,S,S)-1 in absence and presence of Ag(I) and Zn(II) (Figure 5b). Ligand (S,S,S,S)-1 shows a g_{lum} value of -1×10^{-3} , which is in agreement with the previously observed g_{abs} value. An intense CPL response, $g_{\text{lum}} = -1.6 \times 10^{-3}$, is also observed in the case of Zn(II) complexes. Comparison with SAEMS suggests that in this case CPL emission comes from the species with the shortest lifetime, in agreement with the hypsochromic shift in the maxima of CPL (see Figure 4d, brown circles). Moreover, it is clear that the observation of a good CPL signal not only depends on the g_{lum} value. Recently it

has been defined a new parameter, the CPL brightness (B_{CPL}), which takes into account the molar extinction coefficient (ϵ), the emission quantum yield (Φ) and the average g_{lum} .^[25] This parameter is really informative as it provides main photo-physical data and results quite useful for quantifying the overall efficiency of circularly polarized light emitters, allowing the comparison among different molecules. B_{CPL} for ligand (S,S,S,S)-1 has a non-negligible value of $17 \text{ M}^{-1} \text{ cm}^{-1}$, which is good enough for a simple organic molecule and higher than most of described [n]helicenes at that emission wavelength^[26,27] with exception of [7]helicene recently described by Shibata *et al.*^[28] As Figure 5b suggests, B_{CPL} for Zn(II) complex present almost twice ($27 \text{ M}^{-1} \text{ cm}^{-1}$) the initial value, being thus among the highest values previously reported in [n]helicenes.^[25] Owing to the fact that Ag(I) complexes present luminescence quenching, CPL studies were restricted to the (S,S,S,S)-1 in the presence of only two equivalents of Ag(I). Above this amount the response is weak and noisy CPL spectra preclude a reliable estimation of the g_{lum} value. With this caution, the observed g_{lum} value is -3×10^{-3} in agreement with the sign of the ECD for low Ag(I) loadings. Although compound (S,S)-2 is fluorescent no reliable CPL signal could be obtained. It is then estimated to be below 1×10^{-5} . The reason is not clear but probably it can adopt an essentially planar structure in the excited state in which the sulfoxides are the only chiral entities in the molecule. The corresponding absorptions are higher in energy than the corresponding to the conjugated backbone and consequently cannot contribute to the potentially chiral S_1 - S_0 transition.

Finally, we performed theoretical calculations to shed light to the expected double helical geometry of the (S,S,S,S)-1 metal complexes and to correlated the calculated ECD spectrum with the experimentally obtained. Systematic theoretical studies accounting for all these observations are complex for several reasons: i) the complexity of the system, ii) different stoichiometries and metals, and iii) the choice of the best theoretical method to correctly evaluate both oxophilic/carbophilic and π - π stacking interactions. The last point is critical to obtain a reliable conformational landscape, owing to the fact that either underestimated or overestimated interactions may result, depending on the chosen functional and considering dispersion effect corrections. Herein, we adopted M06-2X^[29] functional (see SI for details).

For all these reasons we decided to use calculations just to suggest possible structures compatible with the above observations, mainly in order to check if the system may effectively be optimized in stable double helical structures and if the corresponding calculated ECD spectrum resembles the one experimentally obtained (see SI for a non-exhaustive compilation of all the examined optimized structures, by testing opposite helicities, and different Ag(I) or Zn(II) content). Optimized structures of complexes presumably formed in presence of an excess of metal salts are shown in Figure 6. Thus, (S,S,S,S)-1 ligand is able to incorporate 6 silver atoms coordinated to both the two alkyne arrangements and the four sulfoxide groups at both arms of the skeleton, in a similar way to that observed for previous OPE derivatives.^[21] On the other hand, two zinc atoms were coordinated to the sulfoxide groups

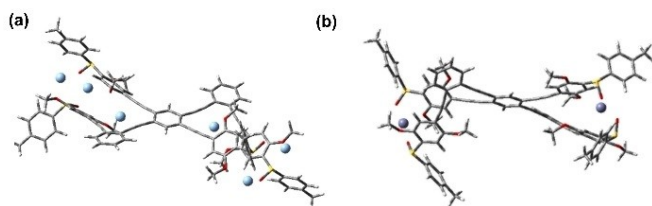


Figure 6. Optimized structures for compound (S,S,S,S)-1 in presence of an excess of a) AgBF₄ and b) Zn(OTf)₂.

giving rise to the metal complex shown in Figure 6b, resembling the structures previously described.^[23] The calculations show that Ag(I) interaction (at least two ions to maintain symmetry) seems to favor *P* helicity, also based on the calculated DFT energy; Zn(II), on the contrary, seems to favor *M* helicity, according to comparison with experimental results (for calculated spectra see Figures S27–S30).

3. Conclusions

In this work we have synthesized two analogues of double helixenes based on multipodal *o*-OPE derivatives, demonstrating that helical *o*-OPE can be designed in the same way as prototypical helixenes, and therefore enriching what we may call the chiral chemical space. Compound (S,S,S,S)-1 presents both oxophilic and carbophilic potential binding sites. In this sense, we have analyzed optical and chiroptical properties in presence of Ag(I) and Zn(II) cations, affording different behaviors depending on the metal. In both cases we observed intensification of ECD and CPL signals when metal complexes were formed. However, while Ag(I) addition promoted inversion of the helicity, showing for the less energetic ECD band a positive sign, the Zn(II) complex maintained *M* helicity with a 4-fold intensity value. On the other hand, the CPL emission for both Ag(I) and Zn(II) showed a more defined and intense peak shifted to the blue. In addition, with the aid of TRES experiments, CPL observed upon Zn(II) coordination, could be attributed to the species with the shortest lifetime.

Experimental Section

Supplementary data associated with this article as well as general information on the experimental details (synthesis, NMR, HRMS, steady state and time-resolved spectroscopy, theoretical calculations) can be found in the supporting information (SI).

Acknowledgements

We thank the Ministerio de Economía y Competitividad (CTQ2017-85454-C2-1-P and CTQ2017-85454-C2-2-P), Ministerio de Ciencia e Innovación (PID2020-113059GB-C21 and PID2020-

113059GB-C22) and Junta de Andalucía (P20.00162) (Spain) for funding and P.R. and A. O. G. also for FPU contracts. Funding for open access charge is acknowledged to Universidad de Granada / CBUA. We also thank Big&Open Data Innovation Laboratory (BODal-Lab), University of Brescia, granted by Fondazione Cariplo and Regione Lombardia, for access to resources of Computing Center CINECA (Bologna), Italy. Support from the Italian MIUR (Grant No. 2017A4XRCA) is also acknowledged.

Conflict of Interest

The authors declare no conflict of interest.

Keywords: chiroptical properties • circularly polarized luminescence • foldamers • helical structures • supramolecular metallofoldamers

- [1] H. Song, M. Postings, P. Scott, N. J. Rogers *Chem. Sci.* **2021**, *12*, 1620–1631.
- [2] J. Zhao, P. Xing *ChemPlusChem* **2020**, *85*, 1511–1522.
- [3] W.-L. Zhao, M. Li, H.-Y. Lu, C.-F. Chen, *Chem. Commun.* **2019**, *55*, 13793–13803.
- [4] K. Dhbaibi, L. Favereau, J. Crassous, *Chem. Rev.* **2019**, *119*, 8846–8953.
- [5] K. Kato, Y. Segawa, K. Itami, *Synlett* **2019**, *30*, 370–377.
- [6] C. Li, Y. Yang, Q. Miao, *Chem. Asian J.* **2018**, *13*, 884–894.
- [7] T. Mori, *Chem. Soc. Rev.* **2021**, *121*, 2373–2412.
- [8] H. Tanaka, M. Ikenosako, Y. Kato, M. Fujiki, Y. Inoue, T. Mori, *Commun. Chem.* **2018**, *1*, 38.
- [9] H. Tanaka, Y. Kato, M. Fujiki, Y. Inoue, T. Mori, *J. Phys. Chem. A* **2018**, *122*, 7378–7384.
- [10] E. S. Gauthier, R. Rodríguez, J. Crassous, *Angew. Chem. Int. Ed.* **2020**, *59*, 22840–22856; *Angew. Chem.* **2020**, *132*, 23036–23052.
- [11] K. Nakamura, S. Furumi, M. Takeuchi, T. Shibuya, K. Tanaka, *J. Am. Chem. Soc.* **2014**, *136*, 5555–5558.
- [12] H. Ito, H. Sakai, Y. Okayasu, J. Yuasa, T. Mori, T. Hasobe, *Chem. Eur. J.* **2018**, *24*, 16889–16894.
- [13] S. Rinaldi, *Molecules* **2020**, *25*, 3276.
- [14] E. A. John, C. J. Massena, J. Casey, O. B. Berryman, *Chem. Rev.* **2020**, *120*, 2759–2782.
- [15] S. Dey, R. Misra, A. Saseendran, S. Pahan, G. Saikat, N. Hosahudya, *Angew. Chem. Int. Ed.* **2021**, *60*, 9863–9868.
- [16] S. P. Morcillo, D. Miguel, L. Álvarez de Cienfuegos, J. Justicia, S. Abbate, E. Castiglioni, C. Bour, M. Ribagorda, D. J. Cárdenas, J. M. Paredes, L. Crovetto, D. Choquesillo-Lazarte, A. J. Mota, M. C. Carreño, G. Longhi, J. M. Cuerva, *Chem. Sci.* **2016**, *7*, 5663–5670.
- [17] P. Reiné, A. G. Campaña, L. Álvarez de Cienfuegos, V. Blanco, S. Abbate, A. J. Mota, G. Longhi, D. Miguel, J. M. Cuerva, *Chem. Commun.* **2019**, *55*, 10685–10688.
- [18] A. M. Ortuño, P. Reiné, S. Resa, L. Álvarez de Cienfuegos, V. Blanco, J. M. Paredes, A. J. Mota, G. Mazzeo, S. Abbate, J. M. Ugalde, V. Mujica, G. Longhi, D. Miguel, J. M. Cuerva *Org. Chem. Front.* **2021**, DOI: 10.1039/D1QO00822F.
- [19] A. Martín-Lasanta, L. Álvarez de Cienfuegos, A. Johnson, D. Miguel, A. J. Mota, A. Orte, M. J. Ruedas-Rama, Maria Ribagorda, Diego J. Cárdenas, M. Carmen Carreno, A. M. Echavarren, J. M. Cuerva, *Chem. Sci.* **2014**, *5*, 4582–4591.
- [20] J.-L. Ma, Q. Peng, C.-H. Zhao, *Chem. Eur. J.* **2019**, *25*, 15441–15454.
- [21] S. Resa, D. Miguel, S. Guisán-Ceinos, G. Mazzeo, D. Choquesillo-Lazarte, S. Abbate, L. Crovetto, D. J. Cárdenas, M. C. Carreño, M. Ribagorda, G. Longhi, A. J. Mota, L. Álvarez de Cienfuegos, J. M. Cuerva, *Chem. Eur. J.* **2018**, *24*, 2653–2662.
- [22] S. Resa, P. Reiné, L. Álvarez de Cienfuegos, S. Guisán-Ceinos, M. Ribagorda, G. Longhi, G. Mazzeo, S. Abbate, A. J. Mota, D. Miguel, J. M. Cuerva, *Org. Biomol. Chem.* **2019**, *17*, 8425–8434.
- [23] P. Reine, A. M. Ortuño, S. Resa, L. Álvarez de Cienfuegos, V. Blanco, M. J. Ruedas-Rama, G. Mazzeo, S. Abbate, A. Lucotti, M. Tommasini, S.

- Guisán-Ceinos, M. Ribagorda, A. G. Campaña, A. J. Mota, G. Longhi, D. Miguel, J. M. Cuerva, *Chem. Commun.* **2018**, 54, 13985–13988.
- [24] M. C. Carreño, I. García, M. Ribagorda, E. Merino, I. Nuñez, S. Pieraccini, G. P. Spada, *J. Am. Chem. Soc.* **2007**, 129, 7089–7100; I. Nuñez, E. Merino, M. Lecea, S. Pieraccini, G. P. Spada, C. Rosini, G. Mazzeo, M. Ribagorda, M. C. Carreño, *Chem. Eur. J.* **2013**, 19, 3397.
- [25] L. Arrico, L. Di Bari, F. Zinna, *Chem. Eur. J.* **2021**, 27, 2920–2934.
- [26] C. Schaack, L. Arrico, E. Sidler, M. Gjrecki, L. Di Bari, F. Diederich, *Chem. Eur. J.* **2019**, 25, 8003.
- [27] C. Schaack, E. Sidler, N. Trapp, F. Diederich, *Chem. Eur. J.* **2017**, 23, 14153.
- [28] T. Otani, T. Sasayama, C. Iwashimizu, K. S. Kanyiva, H. Kawai, T. Shibata, *Chem. Commun.* **2020**, 56, 4484.
- [29] Y. Zhao, D. G. Truhlar, *Acc. Chem. Res.* **2008**, 41, 157–167.

Manuscript received: July 29, 2021
Revised manuscript received: August 24, 2021
Accepted manuscript online: August 25, 2021
Version of record online: September 12, 2021